

Quark spectral functions from spectra of mesons and vice versa

V. Šauli^{1,*}

¹*Department of Theoretical Physics, Institute of Nuclear Physics Rez near Prague, CAS, Czech Republic*

We extract the spectral function of quarks using the QCD functional formalism. The reliability of approximations is controlled by the masses and decays of pseudoscalar mesons. For light quarks, we select the pion; for charm quarks, we choose the ground and excited states of the η_c meson. To this end, we solved the ladder-rainbow approximation of the spectral Dyson-Schwinger equations for quarks coupled to the Bethe-Salpeter equation for the pion and pseudoscalar charmonia. The obtained dynamical charm mass function varies from 1 to 1.5 GeV in the timelike domain, which is significant for narrow charmonium states. This yields a notable response in the bound state spectrum. We obtained purely continuous spectral functions and discussed their connection with confinement.

PACS numbers: 11.10.St, 11.15.Tk

I. INTRODUCTION

Knowledge of QCD correlation functions in the time-like momentum region is crucial for the first-principles determination of hadronic resonances and the understanding of hadron production [1, 2]. In this regard, the analytical continuation of lattice data for propagators to timelike Minkowski space has been challenged [3, 4]. A complementary method to lattice reconstruction is the spectral functional formalism. In this approach, the analytical continuation is performed from the outset using a suitably truncated set of Dyson-Schwinger equations (DSEs), and the equations are solved for spectral functions in Minkowski space. Since the initial spectral study [5], the method has recently been recognized as valuable [1, 6–10] and includes the topic of spectral renormalization - primary or secondary subtractions technique performed at the timelike momentum scale. The Yang-Mills sector of $SU(3)$ gauge theory was considered in Landau gauge [11, 12] bringing new insights for a moderate coupling models. Furthermore, the first primitive solution [7], shows the importance of transverse vertices in strongly coupled pure gluodynamics.

This paper focuses on the quark propagator — particularly the heavy quark propagator — and its spectral function. It offers an alternative explanation for the heavy quarkonium mass spectra by accounting for the often overlooked running quark mass effect. Recall the behavior of the mass function at the naive threshold: the QCD quark mass grows with the timelike scale, which is important for quarkonium physics. Thus, the heavier excited states are effectively composed of quarks that are heavier than those constituting the ground state. In other words, when retardation effects are correctly accounted for in the fully covariant approach of BSEs, the radiative corrections that are responsible for running masses provide the same quarkonium spectrum as is predicted by nonrelativistic quantum mechanics, which includes a phenomenological confining potential in addition to the expected Coulomb term. The nonrelativistic Schrödinger equation with a confining interaction was introduced historically in [13] and used broadly in recent extended studies [14–26] and can effectively replace the quantum field theory effect of running mass.

To determine whether this scenario applies to heavy quarkonia, we employ the DSE for heavy quarks, coupled with the BSE for heavy quarkonia, as was done for quarkonia [27] and many times for the lighter mesons [32–40] where the running quark mass is a critically needed phenomenon. However, we avoid introducing a covariantized form of the confining potential, as was done earlier by the authors in [41, 42]. This would interfere badly with the similar effect stemming from the considered running quark mass. Interestingly, the pion and heavy quarkonia (pseudoscalar charmonia) can be described by nearly the same functional form of the DSE kernel.

In the next section, we describe the calculation scheme for the quark propagator and the BSE. Section III describes the method for BSE solution and for the extraction of the light quark spectral functions. Section IV presents the same but for the pseudoscalar charmonium. We conclude in the last section V.

*Electronic address: sauli@ujf.cas.cz

II. TRUNCATION OF SDES SYSTEM

For the sake of completeness, we will write down all the necessary equations here. The quark propagator S can be parametrized as follows:

$$S(q, \mu) = [A(q^2, \mu) \not{q} - B_q(q^2, \mu)]^{-1} \quad (2.1)$$

where A, B are two scalar functions that completely characterize the quark propagator when the electroweak interaction is turned off. The DSE for the quark propagator in the MOM renormalization scheme can be written as

$$\begin{aligned} A(q^2, \mu) &= a(\mu) - Tr \frac{\not{q}}{4q^2} \Sigma_r(q) + Tr \frac{\not{q}}{q^2} \Sigma_r(q)|_{q^2=\mu^2} \\ B(q^2, \mu) &= b(\mu) + \frac{Tr}{4} \Sigma_r(q) - \frac{Tr}{4} \Sigma_r(q)|_{q^2=\mu^2} \\ \Sigma_r(q) &= i \frac{4}{3} \int \frac{d^D k}{(2\pi)^D} \gamma_\mu S(q-k) \Gamma_\nu(k, q) G^{\mu\nu}(k), \end{aligned} \quad (2.2)$$

where Tr is for the trace over the Dirac indices. The inverse of A is traditionally called the quark renormalization function. The rate B/A represents the renormalization-scheme invariant dynamical quark function $M(q^2)$. The MOM renormalization scheme is known to be particularly useful for evaluating spectral functions and provides a straightforward interpretation of the constants $a(\mu)$ and $b(\mu)$. These constants represent the values of the renormalized functions $A(\mu^2, \mu)$ and $B(\mu^2, \mu)$, respectively. As in the [6] quark selfenergy Σ_r has been regularized dimensionally before the intended subtractions.

The usual routine is to use the "large" spacelike renormalization scale when solving the DSE for the quark propagator to obtain the current quark mass. However, this is an unfavorable choice when solving the DSE for the quark spectral function because it causes numerical convergence to fail. Hence, to renormalize the light quark propagator, we take $\Re a(\mu) = 1$ and $\Re b(\mu) = 300 MeV$ for a small time-like renormalization scale $\mu^2 = 0.5 GeV^2$. The imaginary parts of the functions A and B are read from their upper cut values at $p^2 + i\epsilon$ in the complex plane. In other words, they are not arbitrary, and their values must be found as a solution. If one requires that all renormalization constants be real, then only the real parts of the projected self-energy can be subtracted in Eq. (2.2) to ensure that all renormalization constants are real-valued. To find the absorptive parts, we use the method as developed in the paper [6], i.e., we search for their values by scanning intervals and considering the optimal values as results.

In the Eq. (2.2) G stands for the dressed gluon propagator and $\Gamma(k, q)$ represents the dressed quark-gluon vertex. Their color and Dirac indices are suppressed, and Lorentz indices are omitted unless necessary. Assuming that the full vertices have the same color structure as the classical ones yields the prefactor of $4/3$, which is explicitly shown. The popular Ladder-Rainbow Approximation (LRA) is used and for the product of the quark-gluon vertex Γ and the gluon propagator G we take

$$\Gamma_\nu G^{\mu\nu}(p) = \gamma_\nu N(\xi) \left[-g^{\mu\nu} + \frac{p^\mu p^\nu}{p^2} \right] \int do \frac{\rho_T(o)}{p^2 - o + i\epsilon} - \not{p} \frac{\xi g^2 p^\mu}{(p^2)^2}, \quad (2.3)$$

where ρ_T is the LRA spectral function- a slightly general version of the Landau gauge gluon spectral function. $N(\xi)$ stands for momentum independent constant factor and ξ stands for the usual gauge fixing parameter.

In the Landau gauge, the function ρ_T would provide the effective QCD charge, which falls as $\ln^{-1}[Q/\Lambda_{QCD}]$. Although results already exist for heavy quarks in this approximation, solving the associated coupled DSE for the spectral function and BSE for mesons is extremely difficult. In this report, we do not solve the gluonic spectral DSE or use a running charge in order to reduce the number of numerical integrations. Instead, we have used a simplified following fit for the spectral function

$$\rho_T(o) = -\delta(o - m_g^2) + \delta(o - \Lambda^2), \quad (2.4)$$

with $m_g = 0.6 GeV$ and $\Lambda = 2 GeV$ as found in [7]. Let us mention here, that the undergoing Landau gauge study, which uses more realistic running coupling, lifts the gluonic scales m_g and Λ significantly $m_g \simeq 1.5 GeV$, being thus very close to original estimate [5] for the gluonic mass scale.

The parameters $N(\xi)$ as well as the gauge parameter ξ were varied to find the solution which complies with

1. spectral property of the quark propagator
2. meson properties.

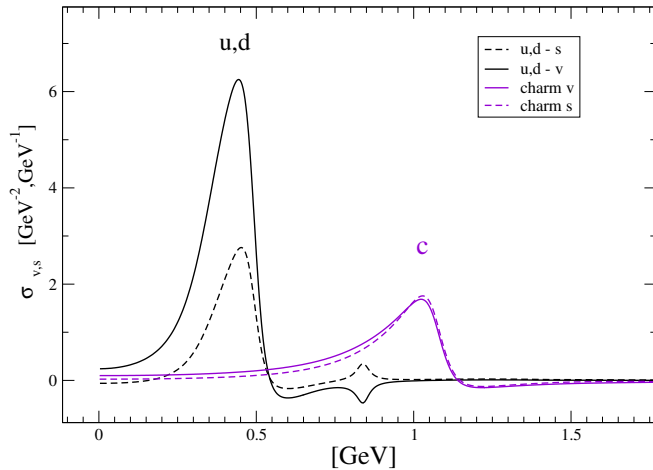


FIG. 1: Quark spectral functions, solid line stands for the functions σ_d , dashed line for σ_s as plotted against energy. The two blobs on the left are for light quarks and the blob on the right is for the charm quark.

To ensure the first point, the DSE is solved for the spectral functions σ for which purpose we follow the method established and described in details in the paper [6]. The method provides a solution to the equation(2.2) in the entire Minkowski space, thereby confirming that the spectral representation for the quark propagator exists in the standard form:

$$S(p, \mu) = \int_0^\infty do \frac{\not{p}\sigma_v(o) + \sigma_s(o)}{p^2 - o + i\epsilon}. \quad (2.5)$$

Two introduced spectral function stands for the dirac and the scalar part of the quark propagator

$$S_v(p^2) = \frac{A(p^2)}{p^2 A^2(p^2) - B^2(p^2)} = \int_0^\infty do \frac{\sigma_v(o)}{p^2 - o + i\epsilon} \quad (2.6)$$

$$S_s(p^2) = \frac{B(p^2)}{p^2 A^2(p^2) - B^2(p^2)} = \int_0^\infty do \frac{\sigma_s(o)}{p^2 - o + i\epsilon}, \quad (2.7)$$

where we have introduced another standard labeling for two scalar propagator functions S_v and S_s ; obviously $S = \not{p}S_v + S_s$. Let us mention that spectral function, likewise the propagator, is a scheme dependent object. In gauge theory like QCD, it nontrivially depends on the gauge fixing parameter as well as on the renormalization point. We will not indicate these dependencies in a further text for brevity.

The desired analytical properties are not automatically guaranteed in QCD as suggested by lattice study [28] and the spectral representation becomes more complicated. We consider the spectral representation to be an approximation, and we minimize the spectral deviation introduced in [6, 7] in order to comply with the point 1. To satisfy point 2 simultaneously, the Bethe-Salpeter equation (BSE) for the pion must produce the correct values of the pion mass, $m_\pi = 140MeV$, and the pionic decay constant, $f_\pi = 90MeV$. This defines the parameter space for modeling the interaction kernel of our LRA, but it also limits the physical renormalization conditions for the quark propagators. Notably, within the truncation presented here it was shown in [6], that the celebrated dispersion relation form [43] for Vacuum Hadron Polarization can be obtained as well as the resulting dispersion relation for the electromagnetic meson form factor [1] appears naturally.

III. RESULTS FOR THE LIGHT QUARK SPECTRAL FUNCTION FROM THE PION PROPERTIES

The homogeneous BSE for mesons is a field-theoretical equation for the quark-antiquark bound state. In a dense notation it reads

$$\Gamma = \int_k S \Gamma S K \quad (3.1)$$

where S is the propagator of the bound state component, Γ is the Bethe-Salpeter vertex function and K is the quark-antiquark-quark-antiquark irreducible interaction kernel. For the pion case, this kernel is taken within the

same approximation as for the DSE in order to consistently preserve the Goldstone character of the pseudoscalar mesons in the chiral limit.

To determine the spectrum, the single-component approximation works well for the ground state [44] as well as for the excited states, confirmed also by the charmonium study [42]. We used the dominant vertex component $\Gamma = \gamma_5 A$ and solved the BSE was solved using the eigenvalue method in complex momentum space.

To get the numerical solution, we introduce a suited auxiliary eigenvalue function, $\lambda(P, A)$. Then, after 3D angular integration and some trivial algebra, the BSE to be solved by method of iterations reads:

$$A(p_E, P) = \lambda(P, A) \int_{-\infty}^{\infty} dk_4 \int_0^{\infty} d\mathbf{k} \frac{\mathbf{k}^2}{\mathbf{p}^2} A(k_E, P) (S_v(k_+) S_v(k_-) (k_E^2 + m_\pi^2) + S_s(k_+) S_s(k_-)) [K_g(k, p) + K_\xi(k, p)]. \quad (3.2)$$

As one can see, the rhs. of the BSE involves the product of the scalar functions $S_v(k_+) S_v(k_-)$ and $S_s(k_+) S_s(k_-)$ evaluated at complex-valued momentum $k_\pm = k \pm P/2$. Here k (or k_E) is a relative real Euclidean momentum, while the total momentum $P_E = (im_\pi, 0)$ in the rest frame of the pion. The propagator S is becoming complex for complex arguments. For an explicit evaluation, we have used the spectral representation (2.7) and implemented an additional integration over the spectral variable in the BSE kernel. However, note the integration factorizes and the both propagator products appearing in the Eq. (3.2) stay real since both propagators in the product are identical. The kernel K_g and K_ξ are usual logs stemming from the "gluon propagator" integrated over the 3d spacelike angles. Thus for instance

$$K_\xi = C_A \frac{g^2 \xi}{(16\pi^3)} \ln \frac{f + 2\mathbf{k}\mathbf{p}}{f - 2\mathbf{k}\mathbf{p}} \quad (3.3)$$

with f defined as $f = k_E^2 + p_E^2 + 2k_4 p_4$.

To solve the quark DSE, we assume that anomalous branch points emerge according to the Schwinger picture of confinement. We found that the branch point is located at the origin of the complex plane rather than at its perturbative value, which is equal to the sum of the pole masses, $m_g + m_p$. However, the pole mass, m_p , does not exist at all (in fact neither does m_g). The quark propagator has a branch cut along the entire positive real semiaxis of the p^2 variable. The resulting spectral functions for the light quarks are shown in the Figure 2. The spectral function for the u quark is equal to that for the d quark because we work in the isospin limit and ignore the electromagnetic interaction.

The broad shapes of both functions $\sigma_{v,s}$ correspond to confined objects- the light quark excitation is always confined inside the pion. It is important to note that the disappearance of the Dirac delta function is a rigid property of the observed solution. The singular peak reappears only when the DSE kernel is made unphysically weak by hand. If one does this explicitly in the DSE for the quark propagator, the same should be done in the BSE. However, this immediately causes one to lose the pion properties of the pionic BSE. This reflects how confinement and chiral symmetry breaking are manifest in the spectral properties of the quark propagator. Consequently, when the pole is absent from the quark propagators, color production thresholds are not generated. This behavior is intuitive and is provided by the solution. There is no need to mimic it by hand, as was done in [45–47] for the purpose of form factor calculations. We obtain confinement of quarks through the solution, both qualitatively and quantitatively.

The following rate of couplings and gauges

$$\frac{g^2 \xi}{N(\xi)} = 3; \quad \frac{4N(\xi)}{3(4\pi)^2} = \frac{16}{3} \quad (3.4)$$

provides one particularly convergent solution in our LRA. Recall that, as observed in [49], extending to other spin mesons is not straightforward in the class of nontrivial covariant gauges. However here for pseudoscalar meson considered here, the deviation from assumed analyticity as established in [6, 7] seems to be vanishing. The value $\sigma^2 = 10^{-6}$ has been achieved and appears to be limited only by the precision of the principal value integral that appears in its definition. Our truncation of BSE/DSE system do not provide excited states as solution of homogeneous equation, which is accordance with broad resonant character of experimentally known π^* . Oppositely, as we describe in the following section, the formalism provides all narrow excited states of pseudoscalar charmonia.

The numerical codes used to solve the BSE are based on an iterative search. We scan the interval of expected mass solutions using 90 iterations for each meson mass. After obtaining the solutions, we store the information and use it to find solutions with greater precision until the desired level of satisfaction is achieved. The final BSE and DSE search codes are available to the public [48].

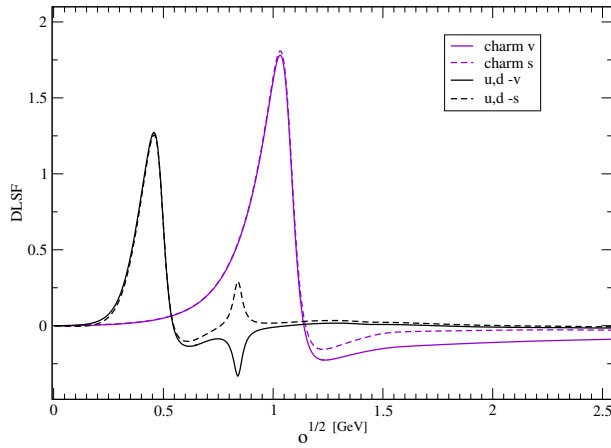


FIG. 2: Dimensionless quark spectral functions $o\sigma_v(o)$ (solid line) and $\sqrt{o}\sigma_s(o)$ (dashed line) for the light and charm quark. At larger (smaller) energy scale the broad peak for the charm flavor (u,d) quark spectral function develops.

IV. C-QUARK SPECTRAL FUNCTION FROM $\eta_c(n)$ QUARKONIA

In this section we describe necessary but minimal changes to get the numerical solution for the charmonium pseudoscalar system. The numerical solution is described below as well.

To find the η_c and its excitations we used the same functional form of DSE/BSE interacting kernel as for the previous calculation of the pion. Furthermore, the dimensionless quantities g and ξ remain exactly the same as in the pion case. According to the flavor non-universality of the quark-gluon vertex, which is a part of our effective coupling a certain changes of the interaction is required to comply with the charm mass scale. This softening is achieved changing the renormalization scale as well as by readjusting the masses that characterize the kernel, which now takes the following values

$$m_g^c = 0.433 \text{ GeV} ; \Lambda^c = 1.442 \text{ GeV}; \quad (4.1)$$

where we add subscript c since a charm flavour.

We fixed the renormalization function and the mass such that $\Re a_c(\mu) = 1$ and $\Re M_c(\mu) = \Re b_c(\mu) = 0.94 \text{ GeV}$ for very low, yet still time-like renormalization point $\mu^2 = 0.13 \text{ GeV}^2$. We also mimicked the effect that could come from higher order skeleton diagrams, such as cross boxes, which carry total momentum dependence. To do so, we insert the following prefactor to mimic the effect beyond LRA:

$$f_\eta = \frac{1}{\sqrt{2}} \sqrt{1 + \frac{M(\eta_c(2))^2}{P^2}}. \quad (4.2)$$

in rhs. of the BSE. Notably, the factor f does not contribute to the ground state.

The coupled system of the DSE for the quark propagator and the BSE for pseudoscalar charmonia was solved in similar manner as for the pion. However, the excited narrow states were also obtained this time. Quite interestingly, the expected "textbook" value of the charm mass $M_c = 1.5 \text{ GeV}$ is reached approximately at the maximum of the dynamical quark mass function $M(p) = B(p)/A(p)$. The mass function in the spacelike domain is smaller than 1 GeV . Additionally, at the scale corresponding to the ground state, the charm function mass function is smaller than expected from nonrelativistic studies. It approaches the value $M(M_{\eta_c}/4) \simeq 1.1 \text{ GeV}$ at the ground state mass scale.

The obtained masses are listed in the Tab I further predicted and not yet observed excited η_c charmonia states we only list here: 5436,6186,7030 MeV,... Our calculations ignore interaction with lighter quarks/meson channels. Therefore these states remain narrow in our approximation and are difficult to compare with a broad resonance observed experimentally. We show our ultimate numerical search for eigenvalue λ and the iteration difference σ^2 (now for BSE) in the figure 3. A single point shown in this figure required one day of heating a recent single-processor machine.

The resulting charm quark spectral functions are added into the fig. 1 for comparison. Since the spectral functions are dimensionful objects, we introduce the dimensionless ones $\sqrt{o}\sigma_s(o)$ and $o\sigma_v(o)$, for a better comparison of the spectral functions of different flavors. These objects are compared in the figure 2. The main rigid property is that

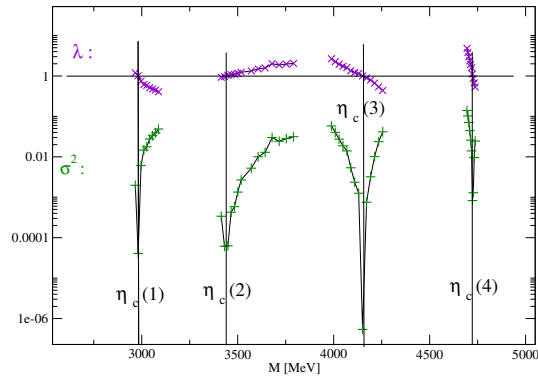


FIG. 3: The eigenvalue λ and the numerical error σ from the solution of BSE the solution for the ground state and the the first three excited state of pseudoscalar charmonium. The definitions can be find in [42], the bound states are for $\lambda \rightarrow 1$ $\sigma \rightarrow 0$ when satisfied simultaneously for the meson mass M .

BSE	EXP.	HLC
2980	2980	3073
3442	3638	3679
4150	—	4171
4720	—	—

TABLE I: Calculated spectrum compared with experimental data (second column). We also compare with the Light front hamiltonian approach results [24] in the third column).

the perturbative on-shell singularity is washed out to into a broad peak, and a heavy a free quark does not exist. The confinement that manifests in the spectral framework of DSEs is the same for light and heavy quarks. The change in the kernel when transitioning from the light to the heavy meson case reveals the importance of the quark-gluon vertex.

The spectra of bottomonia has been obtained in a similar fashion [49], but for the vectors Y instead. However it turns out to be more complicated due to the presence of infrared singularities, which are unavoidable for spin-one bound states. A more comprehensive study of the η_B meson is planned for the future.

V. CONCLUSION

We studied the effect of the running quark mass on the properties of mesons. While its inclusion is necessary to describe the Goldstone character of the pion, we have shown that it is also remarkable for the heavy meson sector. To this end, we solved a coupled set of spectral quark Dyson-Schwinger and Bethe-Salpeter equations to obtain the masses of the desired mesons. Notably, we obtained the masses of excited states of pseudoscalar charmonia. We avoided using relativistic versions or various stringy potentials believed to be "derivable" from gauge-invariant Wilsonian loops. These are unnecessary, as accounting for running quark masses in the equation for bound states fully substitutes their effect. The form of gauge invariant quark propagator as has been established in [50], is very interesting, but far from unique path to observable hadroproductions.

The running coupling and the running of quark masses are unavoidable phenomena stemming from quantum loop corrections in QCD. Specifically, the latter phenomenon was examined in the calculation of $\eta_c(N)$ radial excitations, where the charm mass varied from 1 to 1.5GeV . This turns out to be quantitatively significant and nonnegligible for charmonium physics.

As an added benefit, we obtained spectral quark functions when we solved the DSEs for the quark propagator. At this stage, we should note that there is no urgent need for a purely continuous spectral function, and the use of the constituent quark mass approximation (i.e., the delta function spectrum) provides almost indistinguishable results. Continuous spectral functions do not make the practical life of particle physicists easier; however, they offer a very simple picture of confinement for both light and heavy quarks.

Quarks never live on-shell, nor is their mass ever close to the on-shell mass. The sharp singularity of the perturba-

tive/free quark propagator is completely washed out, and the physical threshold is not presented in a peculiar way. Instead, the imaginary part of the quark propagator gradually grows from the anomalous thresholds, or zero momenta. It goes without saying that the picture can become technically complicated if complex anomalous thresholds arise.

We use the ladder-rainbow approximation, and we acknowledge that the scheme was tuned to minimize deviations from spectrality. Whether the simple picture obtained here survives further improved approximations or extension to other meson flavor sectors can be and will be checked in future studies.

-
- [1] V. Sauli, Phys. Rev. D **106**, 3, 034030 (2022).
 - [2] V. Sauli, Phys. Rev. D **1021**, 014049 (2020).
 - [3] D. Dudal, O. Oliveira, M. Roelfs, P. Silva, Nucl. Phys. B **952**, 114912 (2020).
 - [4] T. Lechien, D. Dudal, SciPost Phys. **13**, 4 097 (2022).
 - [5] J.M. Cornwall, Phys. Rev. D **26**, 1453 (1982).
 - [6] V. Sauli, Few Body Syst. **61** (2020).
 - [7] V. Sauli, Phys. Rev. D **106**, 9, 094022 (2022).
 - [8] E.L. Solis, C.S.R. Costa, V.V. Luiz, G. Krein, Few Body Syst. **60** 3, 49 (2019).
 - [9] J. Horak, J. M. Pawłowski, N. Wink, ArXiv:2210.07597.
 - [10] C. Mezrag, G. Salmè, Eur. Phys. J. C **81** 1, 34 (2021).
 - [11] J. Horak, J. M. Pawłowski, N. Wink, ArXiv:2202.09333
 - [12] J. Horak, J. Papavassiliou, J. M. Pawłowski, N. Wink, Phys. Rev. D **104**,074017 (2021).
 - [13] J. Kogut and L. Susskind, Phys. Rev. D **10** 3468 (1974).
 - [14] Qi Li, Long-Cheng Gui, Ming-Sheng Liu, Qi-Fang Lü, Xian-Hui Zhong, Chin. Phys. C **45** 2, 023116 (2021).
 - [15] Zi-Yue Cui, Hao Chen, Cheng-Qun Pang, and Zhi-Feng Sun, Phys. Rev. D **112**, 056026 (2025).
 - [16] V. Guleria, E. Gebrehana, S. Bhatnagar, Phys. Rev. D **104**, 9, 094045 (2021).
 - [17] Jun-Kang He, Hua-Zhong, Chao-Jie Fan, Phys. Rev. D **103**, 11, 114006 (2021).
 - [18] R. Bruschini, P. González, Phys. Rev. D **101**,1 014027 (2020).
 - [19] S. Bhatnagar, E. Gebrehana, Phys. Rev. D **102**, 9, 094024 (2020).
 - [20] I. Babiarz, V. P. Goncalves, R. Pasechnik, W. Schäfer, A. Szczurek, Phys. Rev. D **100** 054018 (2019).
 - [21] N.R. Soni, B.R. Joshi, R.P. Shah, H.R. Chauhan, J.N. Pandya, Eur.Phys.J. C **78**, 592 (2018).
 - [22] Meijian Li, Yang Li, P. Maris, J. P. Vary, Phys. Rev.D **98** 3, 034024 (2018).
 - [23] Wei-Jun Deng, Hui Liu, Long-Cheng Gui, Xian-Hui Zhong, Phys. Rev.D **95** 3, 034026 (2017).
 - [24] Yang Li, P. Maris, X. Zhao, J. P. Vary, Phys. Lett. B **758**, 118 (2016).
 - [25] D. Becirevic, F. Sanfilippo, JHEP **01**, 028 (2013).
 - [26] Gang Li, Qiang Zhao, Phys. Rev. D **84** 074005 (2011).
 - [27] T. Hilger, C. Popovici, M. Gomez-Rocha, A. Krassnigg, Phys. Rev. D **91** 3,034013 (2015).
 - [28] D. Binosi, R. Tripolt, Phys. Lett.B **801**, 135171 (2020).
 - [29] G. Eichmann, H. Sanchis-Alepuz, R. Williams, R. Alkofer, C. S. Fischer, Prog. Part. Nucl. Phys. **91**, 1-100 (2016).
 - [30] M. Q. Huber, C. S. Fischer, H. Sanchis-Alepuz, Eur. Phys. J. C **80**, 11,1077 (2020).
 - [31] M. Q. Huber, Phys. Rept. **879**, 1-92 (2020).
 - [32] P. Maris, C. D. Roberts, Phys. Rev. C **56**,3369 (1997).
 - [33] V. Sauli, J. Phys. G **35**, 035005 (2008).
 - [34] J. Carbonell, V. A. Karmanov, Eur. Phys. J. A **46**,387 (2010).
 - [35] S. Qin, L. Chang, Y. Liu, C. D. Roberts, D. J. Wilson, Phys. Rev. C **85**, 035202 (2012).
 - [36] T. Frederico, G. Salme, M. Viviani, Phys. Rev. D **89**, 016010 (2014).
 - [37] T. Hilger, M. Gomez-Rocha, A. Krassnigg, Phys. Rev. D **91** 11, 114004 (2015).
 - [38] T. Hilger, M. Gomez-Rocha, A. Krassnigg, Eur. Phys. J. C **77** 9, 625 (2017).
 - [39] T. Hilger, M. Gómez-Rocha, A. Krassnigg, W. Lucha, Eur. Phys. J. A **53** 10,213 (2017).
 - [40] P. Yin, C. Chen, G. Krein, C.D. Roberts, J. Segovia, S. Xu, Phys. Rev. D **100**, 034008 (2019).
 - [41] V. Sauli, Phys. Rev. D **90**, 016005 (2014).
 - [42] V.Sauli,Phys. Rev. D **86**, 096004 (2012).
 - [43] N. Cabibbo and R. Gatto, Phys. Rev. **224** , 1577 (1961).
 - [44] C.S. Fischer, D. Nickel, R. Williams, Eur. Phys. J. C **60**, 49 (2009).
 - [45] T. Branz, A. Faessler, T. Gutsche, M. A. Ivanov, J. G. Körner, and V. E. Lyubovitskij, Phys. Rev. D **81**, 034010 (2010).
 - [46] G. Ganbold, T. Gutsche, M. A. Ivanov, and V. E. Lyubovitskij, Phys. Rev. D **104**, 094048 (2021).
 - [47] S. Dubnicka, A. Z. Dubnickova, M.A. Ivanov, A. Liptaj, Phys. Rev. D **106**, 033006 (2022).
 - [48] author web pages at: gemma.ujf.cas.cz
 - [49] V.Sauli, A study of spin-one bottomonium in the functional formalism in the Feynman gauge, submitted for publication, arXiv:2410.10625.
 - [50] A. Accardi, C. S. R. Costa, A. Signori, ArXiv: 2307.10152 .